CORRELATIONAL ANALYSIS OF LAYERED SUPERCONDUCTING CUPRATES

Vlad Grigore Lascu[*] , Lidia Petrova[**], Cristina Zarioiu[***], Anca Novac[****]
[*] Institute of Solid Mechanics, Romanian Academy, Bucharest, Romania
[**] Joint Institute of Nuclear Research – Dubna, Russia
[***] University of Pitesti, Romania
[****] National Institute for Materials Physics, Bucharest-Magurele, MG-7, Romania
vlad_grigore1947@yahoo.com

Abstract. The paper is a review based on a three level correlational analysis of the behaviour of one compound, of a homologous series and a third interseries multiparametrical analysis, revealing multiple correlation between the critical temperature value and different bond lengths versus the oxygen content. It is described an experimental setup for T_c measurements. A unifying structural scheme of all layered superconducting cuprates is proposed.

Key words: Superconductivity, Layered cuprates, Homologous series, Correlational analysis, Mercury compound

1 Introduction

Since the discovery of high temperature superconductors (HTS) [1] many authors tried to systematize the known information about the HTS structure and related electronic properties in order to understand the physical basic mechanisms responsible for superconductivity. Despite intensive research, the question of how superconductivity arises in high-temperature superconductors is one of the major unsolved problems of theoretical condensed matter physics as of 2008. The mechanism that causes the electrons in these crystals to form pairs is not known. One reason for this is that the materials in question are generally very complex, multi-layered crystals, making theoretical modeling difficult. On the other side, understanding the common features of the structure and related physical parameters is obviously important for challenging the transition temperature, an important parameter for SQUIDs, one of the applications of a quantum effect and having a very large range of uses, from researches in physics, chemistry, biophisics up to bioengineering [2]. The analysed structural data were obtained by refinement programs after applying a series of signal analysis, similar to [3], on the data base obtained by an on-line real-time data acquisition system, similar but a lot more complex than described in [4] and included in the measuring installation. This paper presents a review of the structure information and a unifying analysis of the HTS cuprates.

The general formula of the superconducting copper mixed oxides is $A_mM_2R_{n-1}Cu_nO_{x+\delta}$ with A = Bi, Tl, Hg or Cu; M = Ba, Sr; R = Ca or Y/*RE*, where *RE* is a rare earth element. The m coefficient indicating the number of (AO_δ) adjacent layers is m = 1 for Cu and Hg, m = 2 for Bi and both 1 and 2 for Tl. The n coefficient represents the number of (CuO_2) layers in the unit cell, stacked between two charge reservoir (MO). All the cuprate series have a layered type structure; each series contains a proper alternance of Cu–O planes stacked between the cation (Bi, Sr, Ba, Hg)–O planes and/or simple cation (Y/*RE*, Ca) planes. Finally, the structure consists of alternating blocks with perovskite and rock-salt arrangements. In Figure 1 we revealed the great similarity of this large family. The (CuO_2) layers responsible for superconductivity (SL) are located in the perovskite blocks and their number per unit cell can vary. Actually there were sinthetized Bi/Tl compounds with up to n = 5 and Hg compunds with up to 6 (CuO_2) layers. The rock-salt blocks provide the stability of the structures giving rise to long periodicity along the c axes. In the layered superconducting cuprates, the rock-salt structure blocks play the role of charge reservoir (CRL), as they create the necessary hole concentration in the conducting band for the appearance of superconductivity.Generally the layer sequence is given as follows:

$$(CuO_2)–(MO)–[(AO_\delta)]_m–(MO)–[(CuO_2)–(R)]_n–(CuO_2)–(MO)–[(AO_\delta)]_m–(MO)–(CuO_2) \quad (1)$$

Such a sequence is stable only if the cation–oxygen distance in any given layer is matching the similar distances of the neibour layers, the most important being the distance match with the (CuO_2) and (MO) layers. As first proposed by Goldschmith [5], there is a tolerance factor for the existence of the

perovskite structure and these layers can be stacked if M–O/Cu–O $\approx \sqrt{2}$. As the Cu–O bond length in

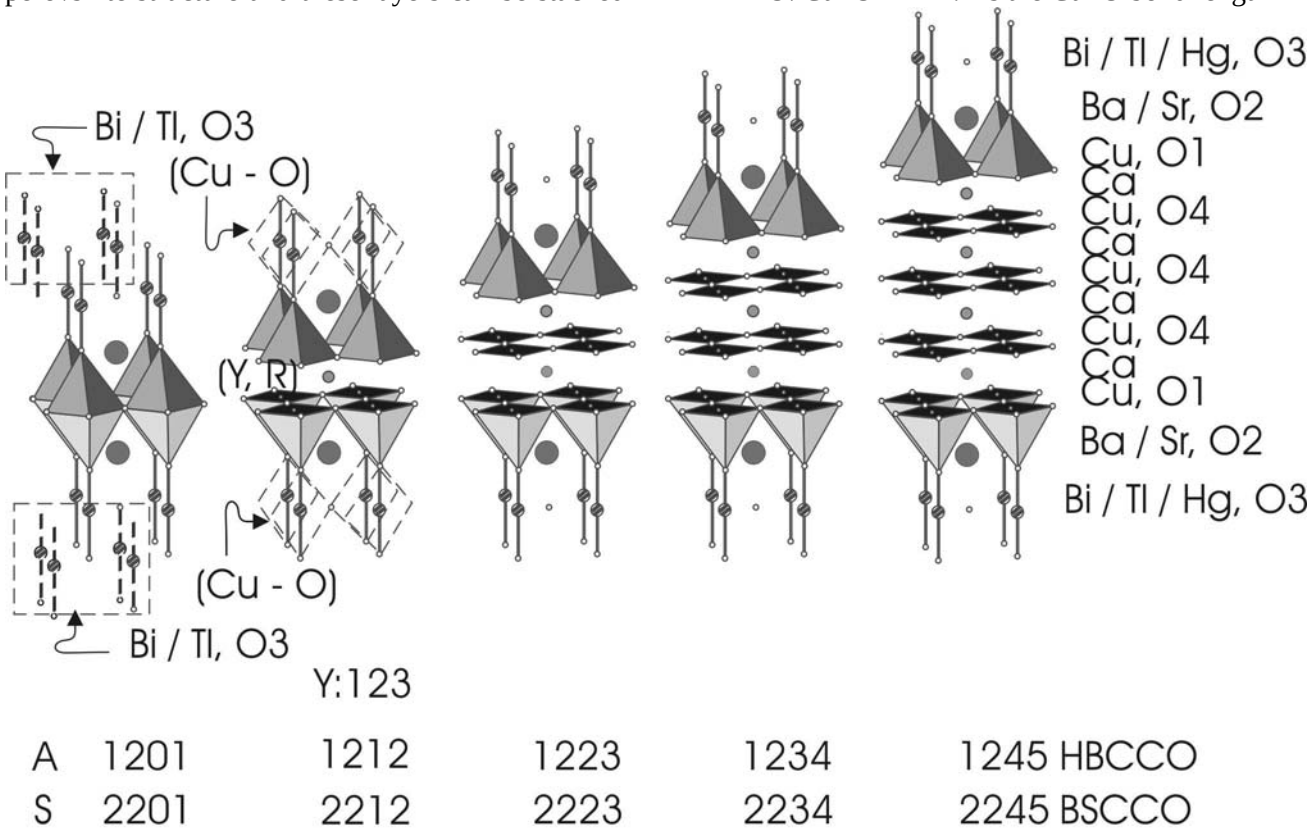

Fig.1 – Homologous series of layered superconducting cuprates.

Table 1. The chemical formulas and the critical temperature of superconducting cuprates.

Compound	T_c (K)
$Y_1Ba_2Cu_{2+n}O_{6+n+\delta}$ (δ = 1- x)	
Y-123 = $Cu_1Ba_2Y_1Cu_2O_{6+x}$ (1212)	92
Y-124 = $Cu_2Ba_2Y_1Cu_2O_{8+x}$ (2212)	82
Y-247 = $Y_2Ba_4Cu_7O_{14+x}$	70
$Bi_1Ba_2Ca_{n-1}Cu_nO_{2n+4+\delta}$	
Bi-2201 = $Bi_2Ba_2Cu_1O_{6+\delta}$	10
Bi-2212 = $Bi_2Ba_2Ca_1Cu_2O_{8+\delta}$	85
Bi-2223 = $Bi_2Ba_2Ca_2Cu_3O_{10+\delta}$	110
Bi-2234 = $Bi_2Ba_2Ca_3Cu_4O_{12+\delta}$	<110
$Tl_mBa_2Ca_{n-1}Cu_nO_{2n+m+2+\delta}$	
Tl-1201 = $Tl_1Ba_2Cu_1O_{5+\delta}$	<10
Tl-1212 = $Tl_1Ba_2Ca_1Cu_2O_{7+\delta}$	85
Tl-1223 = $Tl_1Ba_2Ca_2Cu_3O_{9+\delta}$	120
Tl-1234 = $Tl_1Ba_2Ca_3Cu_4O_{11+\delta}$	104
Tl-1245 = $Tl_1Ba_2Ca_4Cu_5O_{13+\delta}$	118
Tl-2201 = $Tl_2Ba_2Cu_1O_{6+\delta}$	85
Tl-2212 = $Tl_2Ba_2Ca_1Cu_2O_{8+\delta}$	110
Tl-2223 = $Tl_2Ba_2Ca_2Cu_3O_{10+\delta}$	125
Tl-2234 = $Tl_2Ba_2Ca_3Cu_4O_{12+\delta}$	119
Tl-2245 = $Tl_2Ba_2Ca_4Cu_5O_{13+\delta}$	95

$Hg_1Ba_2Ca_{n-1}Cu_nO_{2n+\delta}$	T_c (K)
Hg-1201 = $Hg_1Ba_2Cu_1O_{4+\delta}$	94
Hg-1212 = $Hg_1Ba_2Ca_1Cu_2O_{6+\delta}$	127
Hg-1223 = $Hg_1Ba_2Ca_2Cu_3O_{8+\delta}$	135
Hg-1234 = $Hg_1Ba_2Ca_3Cu_4O_{10+\delta}$	126
Hg-1245 = $Hg_1Ba_2Ca_4Cu_5O_{12+\delta}$	101
Hg-1256 = $Hg_1Ba_2Ca_5Cu_6O_{14+\delta}$	114

the HTS cuprates varies between 1.90 and 1.89 Å, the ideal M–O distance would be 2.69 to 2.80 Å. The $[(AO)]_m$–(MO) sequence forms rock-salt blocks and should have approximately the same distances.

The ionic radii of Bi^{3+} and Tl^{3+} cations are much smaller than those of Ba^{2+} or Sr^{2+}. The mismatch is reduced via cation mixing or large displacements of the *A* cations or oxygen atoms of the rock-salt layers. For example, in Bi / Tl series, this mismatch is giving rise to a uncommensurate superstructure with the modulation of ~26 Å.

For all the cuprates the experimental data give ~3.8 Å for the lattice parameters *a* and *b*, $a \sim b$. The different values for the lattice parameters are due to the different kind of sample preparation technology or measuring methods, but all the values are closed to 3,81 Å for *a* and *b* parameter for the orthorhombic structure and near 5,30 Å for the monoclinic structure. In Table 1 are given the formulas and the corresponding T_c values for HTS cuprates.

The cuprates' structure is based on the perovskite structure, but their unit cell shows a small orthorhombic distorsion. It can be noted that for YBCO this distorsion is essential for superconductivity, the tetragonal compound being, generally, a nonsuperconducting one.

There are some common features of the layered superconductor cuprates structures: a) two types of small distorsions in the Cu–O planes: in-plane and out-of-plane distorsion, both maintaining a closeness to the D_{4h} symmetry; b) single cation layers, without O, separating two CuO_2 layers symmetrically disposed and c) closely spaced Cu–O layers.

Irrespective of the microscopic mechanisms acting in HTS, this analysis should give some insight into the crystal lattice supporting superconductivity. Present paper provides some necessary conditions as we believe them for the superconductivity in cuprates. A series of different factors – such as oxigen content, valence requirements and stoichiometry – must be satisfied, as will be related.

1.2 Formula unit - basic cell

Known superconducting cuprates form homologous series monitored by the number of CuO_2 planes.

In order to get a generic picture of HTS cuprates, it is convenient to define a structural subunit named basic cell of volume $a_0 \times b_0 \times c_0$ with $a_0 \approx b_0$ and containing one formula unit. For $a_0 = b_0$ the basic cell has a tetragonal symmetry D_{4h}, and for $a_0 \sim b_0$ the basic cell will have the symmetry D_{2h} close to symmetry D_{4h}. Furthermore, if the CuO_2 planes are aligned along the *c* direction, having all the Cu atoms with the same projection on the $a_0 \times b_0$ plane, then the unit cell contains one basic cell and the structure is aligned. If the upper CuO_2 planes are horizontally shifted by (1/2, 1/2, 0), then the unit cell will contain more basic cells and the structure is staggered.

For example, Y:123 and HBCCO are aligned and their unit cell contains one basic cell, while Y:124, the first member of BSCCO, TBCCO series are staggered and their unit cell contains 2 basic cells, i.e. two formula units. Therefore, the staggered structure doubles the number of basic cells contained by the unit cell.

1.3 Structure distorsions

Superconductor cuprates are generally not ideal tetragonal compounds with flat oxide planes. Here we discuss two main types of distorsion that may occur, i.e. the *in-plane* and the *out-of-plane* distorsions.

The first refers to the small orthorhombic distorsion of the basic square of the tetragonal structure, which occurs either along the *a*, *b* themselves or along the square diagonal enlarging the unit cell. The diagonal distorsion to orthorhombic symmetry is given by a slight displacement of the corner atoms toward/away from each other along the two diagonals.

The orthorhombic *enlarged* cell is conveniently characterized by an average lattice parameter

$$a_0 = (b + a)/2 \tag{2}$$

and a dimensionless ratio defined as

$$\eta = (b + a)/2(b + a)\,. \tag{3}$$

In addition to the in-plane distorsion of the plane square of the tetragonal structure to form the orthorhombic structure, there is also an out-of-plane distorsion occurring when the oxide layers are no more planar. If the atoms of oxygen are moved upward and downward in equal proportions, the out-of-plane distorsion is *symmetric*, and when they are moved in the same direction relative to the cation, the distorsion is *asymmetric*.

The deviation from the planarity is measured by the layer thickness. Usually, the copper oxide layers are relatively thin, while the Ba, La, Bi / Tl or Hg oxide layers are much thicker. The out-of-plane distorted oxide plane has an average position along the *c* direction, useful for determining interplanar spacing. The deviation from the planarity is measured by the layer thickness, defined as the distance between the uppermost and lowermost atoms in the layer, measured along the *c* direction. Usually, the copper oxide layers are relatively thin, while the Ba, La, Bi / Tl or Hg oxide layers are much thicker.

2 Cuprate series

Now that there were introduced some general features, let us discuss the structure of two perovskites and of the derived compounds of Y, Bi and Hg series. Thallium and mercury form two series of compounds, and yttrium and bismuth only one.

2.1 Perovskite prototypes

Depending on temperature the perovskite $BaTiO_3$ has three crystallographic forms [6]. The TiO_2 layers present in all three structures are similar to CuO_2 layers of cuprates. The high temperature form is fcc. The room temperature form is tetragonal with out-of-plane distorted layers, of about 0,1 Å thickness. The low temperature (below 5°C) form shows the diagonal in-plane distorsion resulting in the orthorhombic structure, while the out-of-plane distorsion is removed.

The mixed valent compound $Ba(Pb_{1-x}Bi_x)O_3$ crystallizes in different systems depending on x values. For $0.05 < x < 0.3$ the structure is orthorhombic of aligned type and the compounds are superconductors. Similar to CuO_2 planes, BaO planes have a very small out-of-plane distorsion (0.12 Å), while BiO planes are thicker (~0.6 Å).

Four similar series of superconducting cuprates with perovskite structure have the general formula $A_mM_2B_{n-1}Cu_nO_x$, where the cations are A = Cu, Bi, Tl, Hg; M = Ba, Sr; and B = Ca, Y, R (rare earth), with $m = 1, 2$ and $n = 1,...6$. These series show mixed oxide valences when the metals have 6s or 6p electron energy close to the $3d(x^2 - y^2)$ Cu – 2p O electron band energy.

2.2 YBCO series

The YBCO series has three members Y:123, Y:124, Y:247. In order to reveal the oxygen content increase, the first superconducting compound $Y_1Ba_2Cu_3O_{7-\delta}$, with $\delta < 0.57$, will be refered as $Y_1Ba_2Cu_3O_{6+x}$, with $x > 0.43$. For the sake of an unified picture, the compound formula can be written as $Cu_1Ba_2Y_1Cu_2O_{6+x}$, which means that it is of 1212-type. This compound has one perovskite type block representing the basic cell. The adding of more (CuO_2) planes into the perovskite block didn't succeed. The unit cell is of aligned type and has three copper oxide planes. The main characteristic is the pair of two (CuO_2) planes, symmetrically disposed relatively to the cation-only plane. The cation = Y or a rare earth (R). The spacing between these two planes is 1.642 Å. These two copper oxide planes are out-of-plane asymmetrically distorted to a rather significant thickness of 0.274 Å. As seen in figure 1, in these two sheets, the cooper atoms Cu1 have a five-fold coordination forming a pyramid, of which four O1 are the in-plane oxygen atoms and the fifth beeing the O2 oxygen from the (BaO) plane. The third (Cu–O) plane is disposed between two (BaO) planes and is perfectly flat with half of oxygen atoms systematically missing and the present ones forming chains along b direction. The Cu2 coordination is distorted square in the a, c plane. For $x < 0.43$, the compound does not show superconducting transition, beeing a tetragonal insulator with no orthorhombic distorsion and having antiferromagnetic properties. For $x = 1$, in the compound $Y_1Ba_2Cu_3O_6$, Cu2 have only two-fold coordination and forms slabs relating Cu–O dumbbells, in a rock-salt type structure.

The second compound Y:124 has one supplementary (CuO_2) plane which separates the original block into two halves, displaced by $b/2$, i.e. two basic cells, and the third compound has three supplementary (CuO_2) planes separating four blocks displaced alternatively by $\pm b/2$, i.e. it has four basic cells.

As Figure 1 shows, the compound Y:123 is a member of the layered family. It can be well assigned to the $m212$ compound, despite the square coordination in the (Cu–O) layer. The oxygen content influence on the superconducting properties will be discussed later.

2.3 Bismuth (Thallium) series

The Bi/Tl and Hg-cuprates form the same type of series, by adding n pairs of (CuO_2) – (Ca) planes. There were synthesized the following compounds: $m201$, $m212$, $m223$ and $m234$, $m245$ and $m256$ with $m = 1$ for Tl and Hg, and $m = 2$ for Bi and Hg.

The chemical formula for the bismuth series can be written as $Bi_2(M)_{n+1}Cu_nO_{2n+4+\delta}$, where M = Ca, Sr, Ba or a combination of them.

We analyse the series with the highest T_c, meaning $Bi_2Sr_2Ca_{n-1}Cu_nO_{2n+4+\delta}$ with n up to 4. The first member (2201) of the series has only one (CuO_2) layer and the lowest T_c of the series. The copper atom is in the center of an octahedron, which is more convenient to consider as a double pyramid. The (CuO_2) plane is almost flat and is common for the two pyramid. Cu1 atoms have six-fold octahedral coordination in the compound 2201.

The second member (2212) of this series, as seen in Figure 1, has a single cation plane which separates the two pyramids. As a result, there are two (CuO_2) almost flat planes, and Cu1 have a five-fold pyramidal coordination, as in Y:123. The single cation layer is Ca and it is surrounded by 8 oxygen atoms arranged as a prism. The following members of the series with n = 3,4,... are obtained by introducing (n-2) planes separating the two pyramids of Cu-O, as schematically shown in Figure 1.

Increasing of n determines the increase of c lattice parameter value. The spacing between the (CuO_2) and (Ca) planes is 1.659 Å. The corresponding cooper ions have a pyramidal oxygen coordination in both cases. The Bi series has a staggered type structure, the unit cell containing two basic cells. The basic cell of this series was reported as tetragonal [7] or orthorhombic [8,9,10,11]. The (CuO_2) layers are rather thin, almost flat, but the

(SrO) planes are thicker with an out-of-plane distorsion.

The perovskite blocks are separated by rock-salt blocks formed by the (BiO) layers. In addition, there was reported a fivefold superlattice structure [9] along the diagonal direction, with the modulation length of 25.8 Å, basically due to the bismuth oxide layers [8]. This distorsion originates in the oxygen distribution. Due to the mismatch of cation–oxygen bonds, in the (BiO) layer the oxygen occupies two types of sites, the rocksalt type and a bridging distorted type [12]. The proper Bi–O bond length should be 2.09 Å for the exchange of one valence unit (v.u.), while in the rock-salt structure this distance is 2.7 Å, corresponding to unsatisfied valence of 0.8 v.u. of oxygen. One way to satisfy the oxygen valence is to alternate regions where the oxygen lies near rock-salt sites with regions where the Bi–O is expanded. In these bridging regions, the distorted substructure allows inserting an oxygen atom between two bismuth atoms. Pushing apart Bi atoms is reflected in the perovskite slabs underneath. If no compensation occured, the perovskite slab would curl up. The second face of the perovskite slab is also lined with a similar (BiO) layer, but with the enlarged region midway between the enlarged regions of the first face. As a result, despite the sinusoidal bending, the perovskite slabs remain globally straight, and can stack to form the crystall. If the superlattice was commensurate, its formula for the compound Bi:2212 would be $Bi_{10}Sr_{10}Ca_5Cu_{10}O_{41}$, but as it is incommensurate with a modulation distance of 4.76 perovskite structure periods, meaning with 4.76*b* (~26 Å), one extra oxygen atom is inserted for every 9.52 Bi atoms, giving $\delta = 0.21$. This excess oxygen raises the copper valence to the value $v_{Cu} = +2.21$, meaning that there are 21% of copper atoms of +3 valence state. The extra oxygen insertion into the (BiO) layer results in a change of the orientation of the Bi^{3+} lone pair of electrons, which causes a decrease of the interlayer distance of two (BiO) adjacent layers and so shrinking of the *c* lattice parameter. The superconductivity in Bi compounds has no relation to structural modulation, as demonstrated for Bi-2212 [13].

A very similar series of cuprates is obtained if Bi positions are occupied by Tl and Sr positions are occupied by Ba, with the mention that thallium form two series with $m = 1$ or 2. Both series have also a staggered type structure. In the thallium compounds (CuO2) layers are thicker and closer together than the corresponding of the bismuth compounds.

We note that the Bi series have two (BiO) layers, for in this series $m = 2$, the second layer being shifted horrizontally by a/2. This presumably is because the lone pair of electrons of Bi+3 needs to be positioned in the interlayer spacing of the (*A*O) double layer. This in turn results in a large interlayer spacing, a weak interlayer Bi–O bonding, and a pronounced layered structure with micaceous properties. The thallium compounds of the homologous series do not show such pronounced micaceous behaviour because interlayer Tl–O bonding is much stronger.

The variation of the Sr / Ca ratio, Bi / Tl and Ca content is reflected by the change of the *c*-parameter. For the 2212 phase, for example, this parameter decreases with increasing of Ca content and increases with increasing of Bi / Tl content [8,14].

It can be noted that, despite the similarity revealed by the XRD spectra (lines positions and intensities) for Tl:2212 and Bi:2212, the structures differ by details, i.e. pseudotetragonal for Tl:2212 and orthorhombic for Bi:2212, underlying that the orthorhombic distorsion is much smaller in Tl compounds than in Bi compounds.

2.4 Mercury series

The Hg series closely resemble that of the monolayer Tl counterparts, except of the occupancy of the O sites. This series have no orthorhombic distorsion allowing most precise determinations of the interatomic and interlayer distances. The (CuO2) layers show a small assymetric, smaller than Y compound. In the (Ba–O) layers the out-of-plane distorsion is about ten times bigger. The unit cell contains one basic cell and the structure is of aligned type. The double layered Hg series is stable only in the presence of Y and it is an insulator. Superconductivity is induced by partially replacinng Y with Ca. The structure is of staggered type, similar to the bismuth series structure. In Hg series, the mismatch between (MO) and (AO) layers is greatly reduced because the occupancy factor of the oxygen sites in the (HgOδ) layers is rather low and most Hg cations have two-fold coordination. The only mismatch remaining in this structure is that beween the (CuO2) and (MO) layers.

3 Critical temperature related with oxygen deficiency and bond legths

It is well accepted that the superconducting properties of HTS compounds are strongly correlated with the existence of mixed valence states of copper, monitored by the oxygen content. The carrier doping of these compounds can be controlled by the preparation technology [15]. The doping effect on T_c is similar with the pressure effect [16]. Concerning the 85 K Bi:2212 superconductor [17,18], the authors reported that the dependency of T_c on the O content is a bell-shaped curve, later surnamed the 'reverted U' function. The maximum T_c value

corresponds to an optimal O content. Since hole concentration can be varied by changing the O content, post-heat treatments under different conditions have been widely adopted to study the effect on superconductivity.

The occupancy factor of the O sites can be submitted to a three level analysis. A first level analysis concerns discussion on the own dependency of each compound, a second one can be performed by studying the variation of Cu valence / O content in the whole homologous series, and a third level analysis will reveal some common features of all the cuprate series. Referring the optimal O content to the series member with the maximal T_c , it could be analyzed the change of the superconducting transition temperature as a function of oxygen doping. Therefore, by using different preparation technologies each compound can be underdoped or overdoped with oxygen relating to the optimal oxigen content. Both under / overdoping induce a decrease of the transition temperature relative to the maximal T_c , the resulting curve being the well known 'reverted U' shape.

3.1 Experimental setup for T_c determination

For the resistivity measurements, which involve making electrical contacts, it is not convenient to move the sample from one holder to another. On the other hand, the understanding of the physical mechanisms involved in the critical state behaviour, as well as many of HTS applications, requires knowledge of the behaviour of the I-V characteristics. We report the development and the use of a rotating sample holder for conductivity studies in small magnetic fields down to liquid helium temperature. We thought it advantageous to design automated measuring system equipped with this sample holder allowing for coarse as well as accurate measurements of the temperature dependence of the sample resistance and, additionally, for measurements of magnetoresistance, current-voltage characteristics and critical currents. Our system is automated from the point of view of data acquisition, realized by the program package DATRISS [19]. The measuring parameters, like temperature, electrical current, its frequency, and magnetic field, are established directly by the user. The low resistance measurements are not easy, especially in the case of ceramic materials like HTS. The commonly used dc four-point methods is based on constant current flow through the sample and measurement of the induced voltage drop in the current direction. The method works fine for well-defined contact geometry and homogeneous samples, except that each experimental point implies two measurements by reversing the sign of the current in order to avoid temf. For this reason we decided to make low frequency (70 Hz) ac measurements using a lock-in nanovoltmeter for detecting the voltage drop on the sample. The block diagram of the constructed setup is presented in Figure 2. In ac measurements a frequency generator controls the current supply and in the same time it gives the reference signal to the lock-in nanovoltmeter. The temperature change is monitored by the REGUL 14 PID (France, CNRS Grenoble) electronic temperature controller using a carbon resistance thermometer (JINR-Dubna, Russia) mounted in a bridge. All the outputs are collected by a Keithley DAS-12 data acquisition card installed in a personal computer. The data acquisition program package DATRISS is a C++ program package [19].

For the measurements of electrical resistivity in order to determine the T_c value, the sample insert can be used in conjunction with a cryostat. The cryostat can be used with liquid nitrogen or liquid helium depending on the minimum required temperature needed for the measurements.

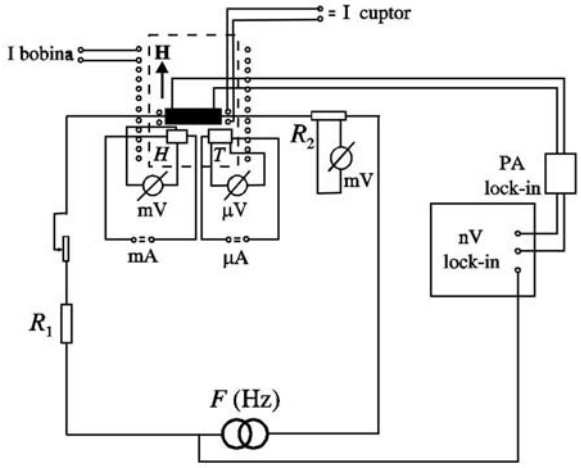

Fig. 2 – T_c measuring block diagram

The insert consists of a calorimeter containing the sample chamber at the bottom of a thin-walled stainless-steel tube allowing a good vacuum. The calorimeter is made of a thin-walled stainless-steel can covered by an external superconductor coil giving the variable weak magnetic field. This can is vacuum fastened on a conical lid greased with Apiezon-N and crossed by the electrical leads inserted in the glass. The sample chamber consists of a radiation shield made of copper and a copper sample holder. The sample holder is a copper plate capable of rotating in a vertical plane, which enables the sample orientation with respect to the applied magnetic field over a range of 360^0 with a resolution of $\pm\ 0.5^0$. The magnitude of the externally applied magnetic field is established by the output of a current controlled power supply in small steps. Field

strength at the sample is measured with a temperature compensated Hall probe that is fixed under the sample inside the copper holder within 0.1 cm from the sample center.

Another problem is the contact resistance which should be low to produce neither Joule heat in the case of the current contacts (especially during critical current measurements) nor Johnson noise in the case of the voltage contacts. These reasons prevented us from using pressure contacts that could make the sample mounting easier and faster. The electrical connections to the sample are made with low frequency shielded copper conductors, and the contact between the sample and the wires are established with silver paint. The wires are taken through holes drilled in the upper copper disk (with a heater) and connected to pins fixed on a teflon ring. In order to avoid any heat flow by the electrical leads we thermally anchored all the leads on the calorimeter lid. During the resistivity measurements the temperature is stabilized or is changing very slowly (for high accuracy measurements) before the sample resistance is measured. The stationary conditions ensure good sample temperature estimate and prevent the existence of a temperature gradient across the sample. Thermal gradients are unavoidable while the temperature is quickly changing, which implies special requirements for the fast resistance measurements. There can be present a temperature gradient across the sample holder, but the sample itself should be kept at one temperature, which means large heat capacity and good thermal conductivity of the sample holder. For these reasons we made the sample holder of copper. The heat exchange between the sample and the holder should be as easy as possible, thus preventing too large temperature difference between them. In fact, there is always a temperature difference between the sample and the holder when the heat is exchanged. The sample should not be enclosed by the holder, thus eliminating a direct heat exchange with the environment by radiation and convection, even in the weak vacuum we use. Because of the presence of these heat flow mechanisms, it is important to be able to estimate the change of the sample temperature caused by them. We have decided to use a thermometer placed in a hole drilled in the road of the sample holder, between the two serial heaters, and a differential thermopower. The first weld of the thermopower is placed in a small hole drilled just near the thermometer and the second one is placed in a hole drilled in the back side of the sample holder disk just in the center. In order to have a good thermal contact with the holder, the thermometer and the thermopower are fixed with Apiezon-N grease. The sample is fixed by the same grease on the sample holder previously covered by a thin layer of GE varnish. The sample holder may be warmed by a resistive heater (two identical symmetrical coils in a serial circuit) and the cooling rate can be changed either by lowering the heater current – in the case of accurate measurement made automatically or by moving the insert above the cooling medium surface (liquid nitrogen usually for HTS) – in the case of a fast measurement.

3.2 First level analysis - *own dependency of the oxygen content of one compound*

Referring to the optimal oxygen content to the series member with the maximal T_c , it could be analyzed the change of the T_c as a function of O doping. Therefore, by using different preparation technologies each compound can be underdoped or overdoped with oxygen relating to the optimal O content. Both under/overdoping induce a decrease of T_c relative to the maximal value , the resulting curve being the well known 'reverted U' shape.

The first level analysis of the YBCO series reveals the tetragonal structure of $YBa_2Cu_3O_{6+x}$ with $x = 0$ compound (or $\delta = 1$ in the formula $YBa_2Cu_3O_{7-\alpha}$) is a nonsuperconducting one (antiferromagnetic semiconductor), as shown by the phase diagram constructed in [20] (Fig. 3). Superconductivity appears only in the presence of the orthorhombic distorsion of the structure with $x > 0.43$ ($\delta < 0.57$). In other words, increasing the oxygen content determines orthorhombic distorsion of the basic oxygen square of (CuO_2) layers and meanwhile the transition from a semiconducting compound to a superconducting one.

$x = 0$ ($\delta = 1$) means maximum O deficiency for the YBCO compound giving the formula $YBa_2Cu_3O_6$. The oxygen atoms of the third copper oxide plane are completely removed and this copper has a linear coordination with the apical oxygen belonging to the (Ba–O). The increase of x determines structure modifications containing two Cu coordinations: pyramidal and linear. For $x = 1$ all the oxygen positions are occupied and the compound is stoichiometric with the formula $YBa_2Cu_3O_7$.

Increasing the oxygen content in the YBCO series causes an increase of the oxidation state of both type Cu atoms. The formal valence of Cu1 in the (CuO_2) layers of the orthorhombic structure increases from +2.18 v.u. up to +2.21 v.u. corresponding to the maximum value T_c of 92 K at $x = 0.9$ ($\alpha = 0.1$). For the stoichiometric compound with $x = 1$, v_{Cu} is fairly smaller. Therefore, this series doesn't show the whole 'reverted U' curve, the overdoped region being absent. The oxygen doping changes also the Cu2 valence, from +1.8 v.u. up to +2.4 v.u. [15].

YBCO was first discovered. The early analysis from the superconductivity point of view revealed that O site occupancy factor (δ) close to 1 is correlated with the maximal T_c. In order to underline the similarity with the other series we decided to discuss the increasing O content as given by doping. In the other series of cuprates, the stoichiometric reference is the formula with missing oxygen in some cation oxide layers and the oxygen doping is reflected by a factor denoted by δ with the big difference that these

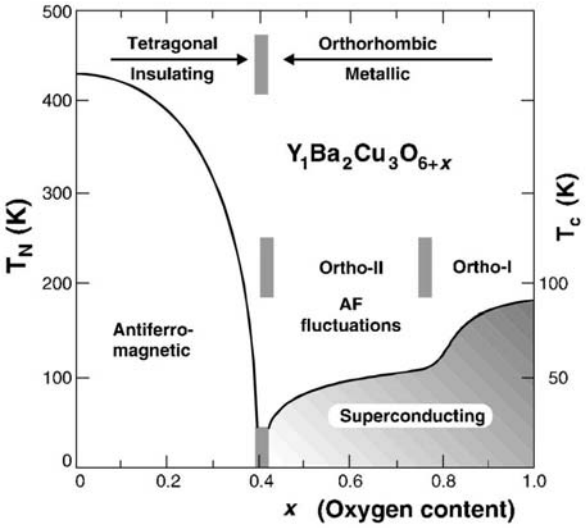

Fig. 3 – Phase diagram of the $Yba_2Cu_3O_{6+x}$ *system versus the oxigen content, x in the* Cu1O1 *layer* [19].

series are analysed as function of increasing this factor. The O content dependence of the Cu valence cannot be directly measured, and the theoretical approach of calculation could differ. In order to make a consistent analysis, we present the results obtained on the Hg series, as the evaluation of Cu valence was made in the same approach for all the compounds and the tetragonal structure allows a high resolution refinement.

The Hg cuprates have similar structure with Tl monolayered homologous series, but the orthorhombic distorsion is absent. The main difference is given by the O content of (HgO_δ) and (TlO_δ) layers. The stoichiometric formula is given for absence of the O atoms in the mercury plane. The extra O atoms of the (HgO_δ) planes ocupy the interstitial position situated in the center of the mercury square. The great importance of the (HgO_δ) layers concern their role of charge reservoir, the presence of these interstitial O atoms changing the valence state of the Cu situated in the (CuO_2) layers. Due to the reduced occupancy number of this position, the O atoms are weakly bonded with the Hg cations, but they have a strong influence upon the other bond lengths. Based on the very weak linear change of the in-plane Cu–O length in (CuO_2) layer given by the O doping, it was concluded that this bond is very strong. On the other side, for the compound Hg-1212 the dependence on δ of the apical distances Cu–O and Hg–O show a minimum, respectively a maximum [18] which are related with the maximal T_c via optimal δ value obtained from the 'reverted U' curve [17]. The O doping has a double effect of opposite sign on the Ba polyhedron. On one hand, there is a mass effect given by the increasing of the coordination number, thus the volume of coordination polyhedron of the Ba cations. At the same time, there is a bonding effect. The O insertion strengthens the bonding, resulting in a decrease of unit cell volume. For $0 \le \delta \le 0.2$ the mass effect prevails and the Ba–O (apical) distance increases. In order to accomplish this diplacement, the apical O and the Ba cation move away from each other decreasing the apical distance Cu–O. For $\delta \ge 0.2$ the bonding effect prevails, the Ba–O (apical) decreases, the apical O and the Ba cation move toward each other, and the apical distance Cu–O increases. Therefore, the O insertion in the (HgO_δ) layer induces the displacement of the apical O linked to the Cu and the Hg cations. Since the displacement occurs via Ba cations, by increasing the O doping the apical Cu–O moves first toward the Cu cation and then away, as a result of the two opposite sign effects. The structure having the shortest Cu–O apical distance seems having the maximum T_c values.

For the Y-123, the apical Cu–O varies from 2.42 Å for $x = 0.5$ to 2.28 Å for $x = 0.9$ and to 0.32 Å for $x = 1$. As the highest value $T_c = 92$ K is reached for $x = 0.9$ the same correlation between the apical distance Cu–O and T_c values can be resumed.

3.2 Second level analysis - *variation of Cu valence / O content in the whole homologous series*

The second level analysis we will perform for the monolayered Hg series concerning the relevant interatomic / interlayer distances relation with the O doping, in correlation with T_c. For each compound of the series, the O content can be varied in a wide range, from underdoped to overdoped composition. Figure 4 shows the 'inverted U' curves obtained for the first three monolayered Hg compounds.

For Bi/Tl and Hg series the T_c value increases with the number n of the (CuO_2) layers up to $n = 3$, afterwards it decreases, but the $n = 5$ Tl compound and the Hg compound with $n = 6$ show unexpected high T_c, as mentioned by the authors [24].

3.3 Third level analysis - *multiparametrical*

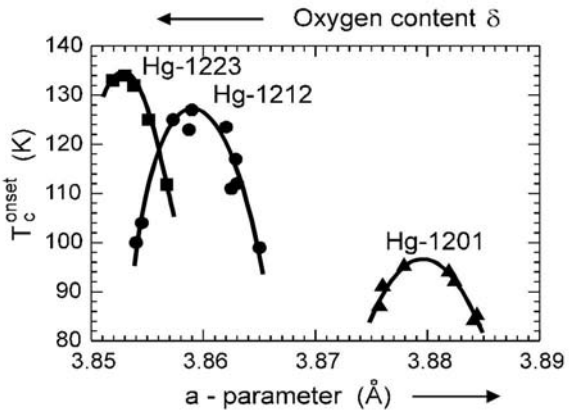

Fig. 4 – The 'reverted U' shape function for the first compounds of the mercury series [17].

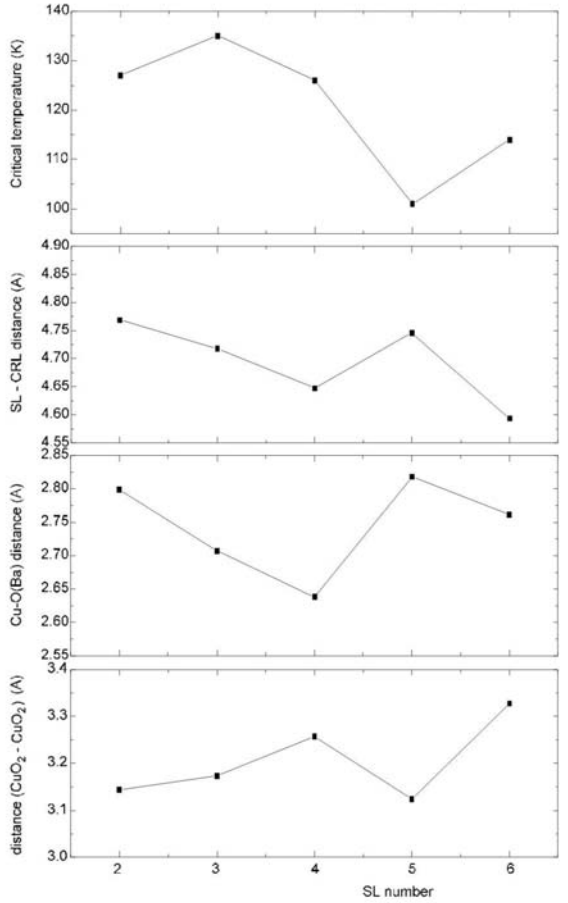

Fig. 5 – The correlations between the T_c and some interlayer distances in the mercury series. Note the unusual behaviour of the compounds Hg-1245 and Hg-1256.

This analysis we will perform on the *m*212 members. Figure 5 shows the dependence of the Cu–O apical distance, the separation between the (CuO_2) layer and (Hg–O_δ) denoted as SL–CRL distance between two neighbouring (CuO_2) layers (separated by the single cation layer) versus T_c value. These correlations could be just an observation, without being generated by the mechanism of superconductivity acting in these layered superconductors. However, the shortening of the distance between two superconducting layers (CuO_2)–(CuO_2) for increasing value could be a hint for a limitation of the T_c in this type of layered superconductors. We remember that for Hg-1212, the minimum of the (Cu–O) apical distance seems to be correlated with the maximum of the critical temperature [18], but between the members of the Hg series, this distance does not seem to be highly correlated.

The interseries analysis made on the *m*212 compounds shows again a possible correlation with T_c. As shown, two of the important distances are raising, but the interlayer separation between two neiboring Cu–O superconducting layers is drastically shortening as the critical temperature exhibited by the *m*212 component is going up.
The correlations shown in Figure 6 could be just an observation, without being generated by the mechanism of superconductivity acting in these layered superconductors. However, the shortening of the distance between two neighbor SL layers (CuO_2)–(CuO_2) for increasing *m* value could be a

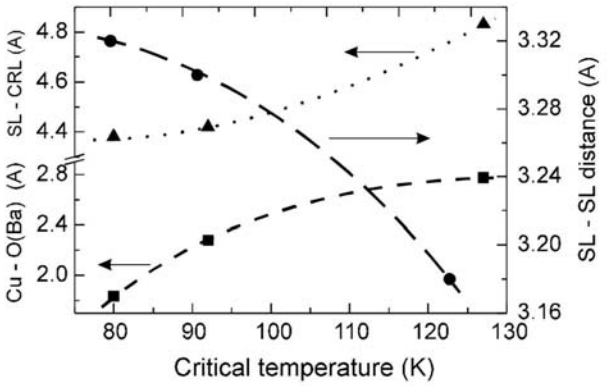

*Fig. 6 – Interseries correlations for the m*212 *compounds:* Bi/2212, Y-1212 *and* Hg-1212.

hint for a limitation of the critical temperature in this type of layered superconductors. We remember that for Hg-1212, the minimum of the (Cu–O) apical distance seems to be correlated with the maximal value of the critical temperature [18], but between all the members of the Hg series, this distance does not seem to be highly correlated.

4 Conclusion

This paper is proposing a unifying structural scheme of all layered superconducting cuprates. Based on a

three level analysis of the superconducting cuprates the review reveals multiple correlation between the critical temperature value and different bond lengths via the oxygen content for yttrium, bismuth and mercury mixed oxides HTS. It would be interesting to apply this analysis on the series of superconductors without Cu, e.g. the newest layered compounds LaOFeP and $LaO_{1-x}F_xFeAs$ [25, 26].

References

[1] J.G.Bednorz, K.A.Müller - *Z.Phys.* **B64**, 189 (1986)
[2] *Proc. WSEAS Int.Conf. BIO'05, Session Biomagnetometer SQUID*, Greece, 206 (2005)
[3] V.Slavov, T.Tashov - Proc. 5th WSEAS Int.Conf. ICOSSE'06, Spain, 228 (2006)
[4] V.N.Ivanovic, R.Stojanovic, S.Jovanovski - *Proc. 6th WSEAS Int.Conf. CSECS'07*, 379 (2007)
[5] V.M.Goldschmith - *Geochemische Verteilungsgesetze der Elemente* VII, VIII, 28 (1927)
[6] R.W.G.Wyckoff - *Crystal Structures*, Vol.2, Wiley, N.Y. (1960)
[7] H.W.Zandbergen, Y.K.Huang, M.J.V.Menken, J.N.Li, K.Kadowaki, A.A.Menovsky, G.van Tendeloo, and S.Amelinckx - *Nature (London)* **332**, 620 (1988)
[8] J.Zhang, H.Shibahara, D.J.Li, L.D.Marks, J.B.Wiley, S.J.Hwu, K.R.Poeppelmeier, S.N.Song, J.B.Ketteson, B.Wood - *Northwestern Univ. preprint* (1988)
[9] D.R.Veblen, P.J.Heaney, R.J.Angel, L.W.Finger, R.M.Hazen, C.T.Prewitt, N.L.Ross, C.W.Chu, P.H.Hor, R.L.Meng - *Nature (London)* **332**, 334 (1988)
[10] E.A.Hewat, M.Dupuy, P.Bordet, J.J.Capponi, C.Chaillout, J.L.Hodeau, M.Marezio - *Nature (London)* **332**, 153 (1988)
[11] D.G.Xenikos, P.Strobel - *Physica* **C248**, 343 (1995)
[12] Y.Le Page, W.R.McKinnon, J.M.Tarascon, P.Barboux - *Phys.Rev*.**B40**, 6810 (1989)
[13] G.Calestani, G.Salsi, M.G.Francesconi, R.Masini, L.Dinesso, A.Migliori, X.F.Zhang, G.van Tendeloo - *Physica* **C206**, 33 (1993)
[14] T.Watanabe, T.Fuji, A.Matsuda - *Phys.Rev.Lett.***79**, 2113 (1997)
[15] X. Sun, W. Wu, L. Zheng, X. Zhao, L. Shi, G. Zhou, X.G. Li and Y. Zhang - *J.Phys.: Condens.Matter* **9**, 6391 (1997)
[16] M.Marezio, J.J.Capponi, P.G.Radaelli, P.P.Edwads, A.R.Armstrong, W.I.F.David - *Eur.J.Solid State Inorg.Chem.***31**, 843 (1994)
[17] W.A.Groen, D.M.Leeuw - *Physica* **C159**, 417(1989)
[18] J.B.Torrance, Y.Tokura, A.I.Nazzal, A. Bezinge, T.C.Huang, S.S.Parkin - *Phys.Rev.Lett.* **61**, 1127 (1988)
[19] Anca Novac, A.S.Nikiforov, V.G.Lascu, A.Dascalu, C.Nichitiu - *Proc.2nd Int.Conf. AMSE "SYS'94", Lyon*, 141 (1994)
[20] J. Rossat-Mignod, L.P.Regnault, P.Bourges, C.Vettier, P.Bourlet, and J.Y.Henry - *Physica* **B186-188,** 1 (1988)
[21] M. Karpinen, A.Fukuoka, L.Niinistö, H.Yamauchi - *Supercond.Sci.Technol.* **9**, 121 (1996)
[22] J.J.Capponi, J.L.Tholence - *private communication* (1995)
[23] M.-H. Whangbo, C. C.Torardi - *Science* **7**, 1143 (1990)
[24] Q.Huang, O.Chmaissem, J.J.Capponi, C.Chaillout, M.Marezio, J.L.Tholence, A.Santoro - *Physica* **C227**, 1 (1994)
[25] Y.Kamihara, H.Hiramatsu, M.Hirano, R.Kawamura, H.Yanagi, T.Kamiya, H.Hosono - *J. Am. Chem. Soc.* **128**, 10012 (2006)
/26/ H.Takahashi, K.Igawa, K.Arii, Y.Kamihara, M.Hirano, H. Hosono - *Nature* **453**, 376 (2008).